International Journal of Biological Macromolecules 192 (2021) 72–81

Contents lists available at ScienceDirect

International Journal of Biological Macromolecules

journal homepage: www.elsevier.com/locate/ijbiomac

Bio-conjugation of anti-human CD3 monoclonal antibodies to magnetic nanoparticles by using cyanogen bromide: A potential for cell sorting and noninvasive diagnosis

Nastaran Moradi [a], Samad Muhammadnejad [b], Hamid Delavari [c], Negin Pournoori [d,e], Mohammad Ali Oghabian [e,*], Hossein Ghafouri [f,g,**]

[a] Department of Biochemistry, University of Guilan, Rasht, Iran
[b] Gene Therapy Research Center, Digestive Diseases Research Institute, Tehran University of Medical Sciences, Tehran, Iran
[c] Materials Engineering Department, Tarbiat Modares University, Iran
[d] Biomarker Imaging and Analysis Group, Research Center for Molecular and Cellular Imaging, Tehran University of Medical Sciences, Iran
[e] Department of Medical Physics and Biomedical Engineering, School of Medicine, Tehran University of Medical Science, Tehran, Iran
[f] Department of Biochemistry, Faculty of Science, University of Guilan, Rasht, Iran
[g] Department of Marine Sciences, The Caspian Sea Basin Research Center, University of Guilan, Rasht, Iran

ARTICLE INFO

Keywords:
Anti-CD3 antibody
Cell sorting
Conjugation
Cyanogen bromide (CNBr)
Magnetic-activated cell sorting (MACS)
Magnetic nanoparticles (MNPs)

ABSTRACT

The conjugation of monoclonal antibodies with superparamagnetic iron oxide nanoparticles (SPIONs) has appeared as a potential multifunctional clinical tool, which can effectively diagnose cancers and monitor their treatment, specifically. Despite the presence of different methods for conjugating antibodies to iron oxide nanoparticles, novel cost-effective and simpler conjugation techniques should be performed in this regard. In current study, an anti-CD3 monoclonal antibody was conjugated to the Fe3O4 coated by carboxymethyl dextran (CMD) using cyanogen bromide (CNBr). Moreover, EDC/NHS techniques were applied as a positive control. The experimental results showed that the Conjugation was performed and the presence of the antibody conjugated to the MNPs in human xenograft tumors was confirmed using Prussian blue (PB) staining, following magnetic resonance imaging (MRI), 30 min after injection. This conjugation method was shown to be able to separate CD3+ T lymphocytes efficiently from whole blood with high purity. Accordingly, this type of bio-conjugation method can be utilized in the future for cell sorting, and can be applied for adopted cell therapies such as CAR-T cell (Chimeric antigen receptor T cell) therapy, as well as targeted MRI imaging.

1. Introduction

The development of the conjugation strategies [1] of high-quality nanoparticles (MNPs) remains a challenge and essential requirement for their application in biomedicine [2]. Additionally, the conjugation of monoclonal antibodies [3,4] with SPIONs is considered as a potential multifunctional clinical tool [5] which is effective in diagnosing [6] and treating cancer [7,8]. Recently, various methods [9,10] are available for conjugating [11] antibodies with MNPs although many researchers aim to find a more cost-effective and easier technique.

Standardized bio-conjugation methods such as EDC/NHS [12,13] are one of such techniques, which involve the modification of reactive groups on MNP surface like amino and carboxyl groups, which can be coupled to the amino acid side chains of the antibody through covalent bonds [14]. It is a commonly used method [15] because of its high stability and covalent bonding to the metal surface, while in some research aggregation and polymerization are reported [16]. Biotinylation is a determinate procedure of labeling antibody molecules for multiple applications in life science research [17]. However, the use of avidin in immunocytochemical detection systems faces two significant problems [18]. At neutral pH, due to have a high isoelectric point of about 10, it is positively-charged. Thus, it may be non-specifically attached to the structures with negative charge such as nucleus. The second problem is that avidin is a glycoprotein, which reacts with the molecules such as lectin through carbohydrate fraction. The physical behavior of the antibody such as its solubility or aggregation can be

* Corresponding author.
** Co-corresponding author.
E-mail addresses: oghabian@sina.tums.ac.ir (M.A. Oghabian), H.ghafoori@guilan.ac.ir (H. Ghafouri).

https://doi.org/10.1016/j.ijbiomac.2021.09.129
Received 23 June 2021; Received in revised form 9 September 2021; Accepted 18 September 2021
Available online 2 October 2021

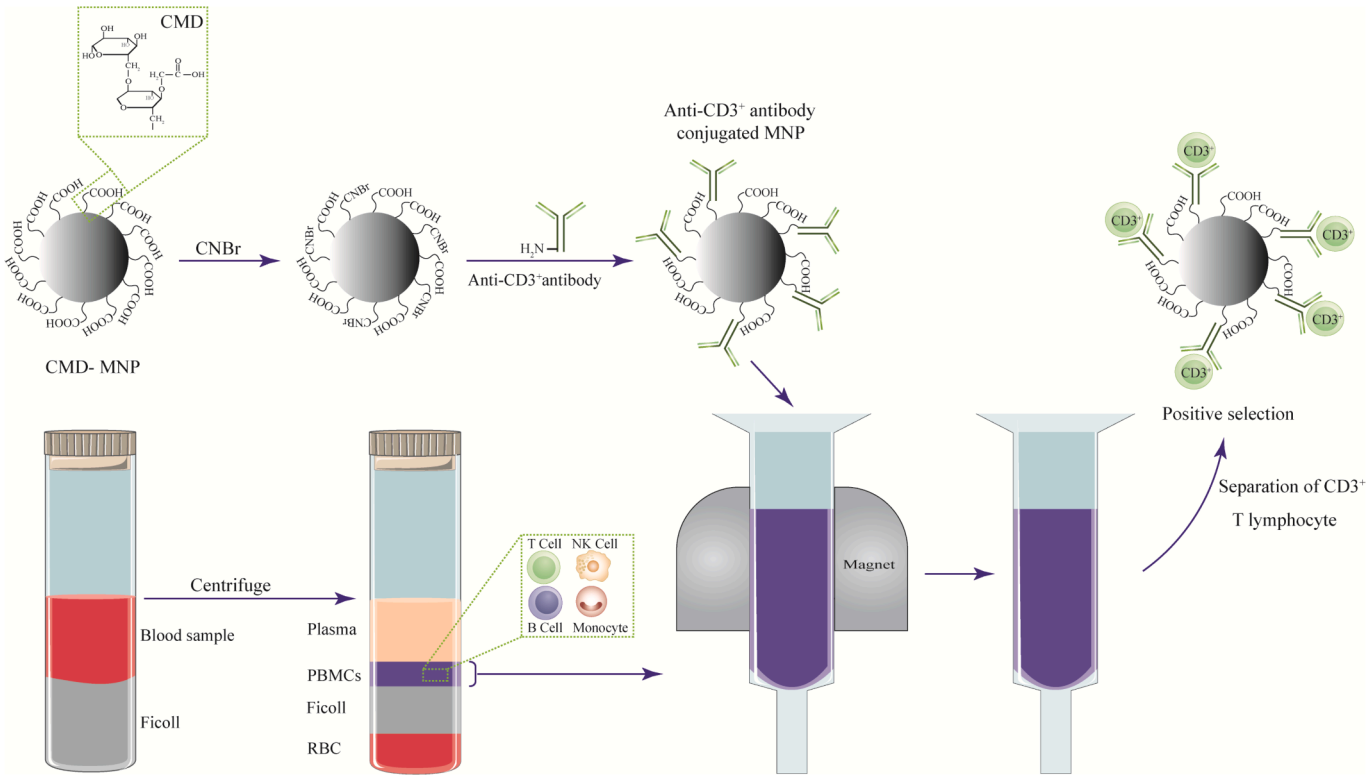

Fig. 1. Schematic description of the used suitable technique for separating target cells from a set of heterogeneous ones by the conjugation process of antibody to microbead and their separation by using MACS.

altered by the excessive biotinylation of lysine residues. Due to the hydrophobicity of biotin and elimination of surface charge by the lysine residues of biotinylation, the protein surface becomes more hydrophobic significantly when attaching multiple biotins. The protocol should be adjusted to reduce biotinylation stoichiometry. A novel solution is using cyanogen bromide as a linker in this conjugation [19], but it hasn't been investigated completely so far. In the present study this method is evaluated in terms of conjugating the antibodies on the MNP surface by using cyanogen bromide strategies. This conjugation type is affordable and the test is fast up to 4 h because of high stability and covalent bonding to metal surface. Further, it does not aggregate and remains stable. High dispersion, great magnetization, stability under physiological conditions, and capacity for binding to biological molecules can be noted as the appropriate functions of the method [20].

T cells can be recognized from other lymphocytes due to the existence of a specific protein (or receptor) on their cell surface, $CD3^+$ T lymphocytes. Among this CD3+ sub-population, 40–75 and 30–45% are CD8+ cytotoxic T lymphocytes (CTLs) and CD4+ helper T cells (Th). [2]. Indeed, CD3 is expressed on the surface of T cells at all stages of its maturing so it has been utilized to detect lymphocytes in tumor samples [3]. Therefore, the tumor-infiltrating lymphocytes and positive T cells can be isolated and labeled by using anti-CD antibodies.

In the medicine, the produced bio-conjugates can be applied for cell sorting, as one of the most important uses of adopted cell therapy such as CAR-T cell therapy [21], as well as developing targeted contrast agents for MRI imaging. Cell isolation is introduced as an useful tool in terms of several aspects such as pathology, clinical diagnosis, cloning, and many other biological methods although adoptive cell therapy is now considered as one of the most important applications of cell sorting, which is known as cellular immunotherapy [22]. The other includes tumor-infiltrating lymphocyte therapy (TIL), which removes the normal T cells which have previously penetrated patients' tumors, and then activates and expands the cells. [23-25]. Today, cell therapies are evaluated both alone and in combination with other treatments in many types of cancer during clinical trials [26].

However, there are many methods such as cell separation [1], fluorescence-activated cell sorting (FACS) [27], density gradient centrifugation [28], immunogenicity cell isolation [29], microfluidic cell sorting [30], electrophoresis [31], and magnetic-activated cell sorting (MACS) [32,14]. MACS is one of the most efficient, cost-effective, and less time-consuming cell separation techniques [33]. In the system, SPIONs are utilized due to cost-effectiveness synthesis and low toxicity. The MNP functionalization is considered as an important strategy for conjugating to biological active residues [34–37].

Molecular imaging is another technique, which is used as a powerful tool to detect biological changes at cellular level and has significantly improved research in the biomedicine field [39,40] such as immunology [38]. Nowadays, molecular MRI imaging detects specific biological molecules by contrast agents and has become popular in molecular imaging due to its benefits such as non-invasiveness, high soft-tissue contrast, and excellent spatial resolution. Based on the results of the previous studies, MNPs are utilized as imaging agents in diagnosing cancer [39], apoptosis [40], and cell migration [41] because of increasing MR signal. The present study tried to provide an optimal and cost-effective method for separating TCD3+ cells from PBMC ones, which can be applied to isolate TIL cells for the clinical purposes using CAR-T cell. In addition, EDC/NHS was used as a positive control and the performance of cyanogen bromide was compared. The Fe_3O_4@CMD-CD3-labeled T cells can be effectively detected in a NOG mouse model through using in vivo MRI. The study aimed to assess whether this conjugation method using cyanogen bromide can provide a microbead for utilizing in cell sorting to CAR-T cell therapy in the future and develop targeted contrast agents for MRI imaging, which is a non-invasive way to distinguish CD3+ lymphoma cancer cells.

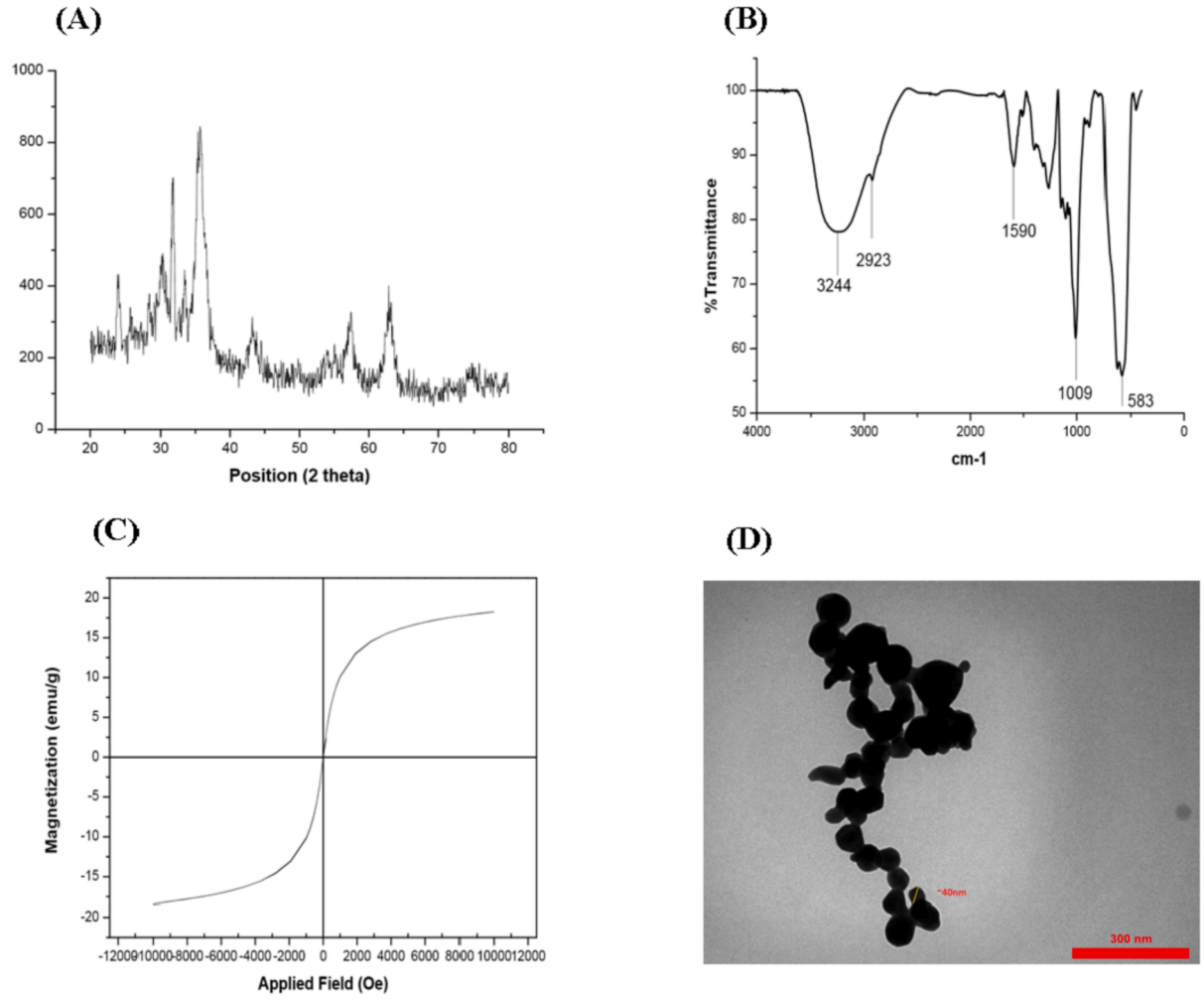

Fig. 2. A) The crystallinity and phase structure of the product were examined through using the XRD pattern analysis and the broaden peaks in the XRD pattern suggested the small particle size of the product. The mean crystallite diameter of the product was estimated by using the Debeys-Scherrer equation as 44 nm which was confirmed by the TEM images. B) The attachment of the CMD on the Fe_3O_4 surface was established through FTIR spectroscopy. C) The magnetic characteristic of MNPs was measured through using VSM demonstrated that all of the MNPs were superparamagnetic at RT with no hysteresis. D) The morphological structure of the NPs was obtained by using a TEM.

2. Materials and methods

2.1. Chemicals

Chemicals were purchased from Sigma, and Aldrich, (3-(4,5-dimethylthiazol-2-yl)-5-(3-carboxymethoxyphenyl)-2-(4-sulfophenyl)-2H-tetrazolium) (MTS) and anti-CD3 monoclonal antibody were prepared from Sigma (USA) and Sina Biotech (Tehran, Iran).

2.2. Conjugating anti-CD3 monoclonal antibody to magnetic microbeads

To this purpose, MNP was purchased from Teb-o-Sanat Rahyab (TOSR) Corporation (Iran) as microbeads that consisted of a Fe_3O_4 core coated by dextran with the molecular mass of 10 kDa. In order to conjugate anti-CD3 to microbeads, 1 mL of 5 mg/mL iron microbeads was mixed with 0.3 μg of cyanogen bromide in 50 μL of acetonitrile and stirred about 10 min at room temperature (RT). In addition, the pH of microbead was set about 10.5 by adding 0.01 g of sodium carbonate (Na_2CO_3) to solution. Further, the pH of solution was reduced to about 8.5 by pouring 0.012 g of sodium dihydrogen phosphate (NaH_2PO_4) and antibody was added. In this regard, 75 μL of 250 μg/mL antibody was diluted to 500 μL, around 50 μL of which was gradually added to activated microbeads at each 30 s. After one hour at RT, 0.003 mg of glycine was added into the mixture in the refrigerator for 4 h to terminate the reaction. Then, separation process was performed in a MACS column.

2.3. Conjugating anti-CD3 monoclonal antibody to MNP by using EDC-NHS

To this end, 10 mM of NHS and 26 mM of EDC were solved in 0.1 M 2-(N-morpholino) ethane-sulfonic acid (MES) buffer (pH = 6.2), followed by adding to MNP and shaking for 2 h at RT. Additionally, the solution was loaded into the MACS column and particles were washed twice with MES buffer (pH = 6.2). Further, 0.45 mg of anti-CD3 monoclonal antibody was added to the active particles and shaken for 4 h to eliminate the excess antibody. Furthermore, the mixture was separated by using MACS and rinsed three times with 1 mL of PBS buffer. Then, glycine was poured to stop the reaction and incubated for 30 min.

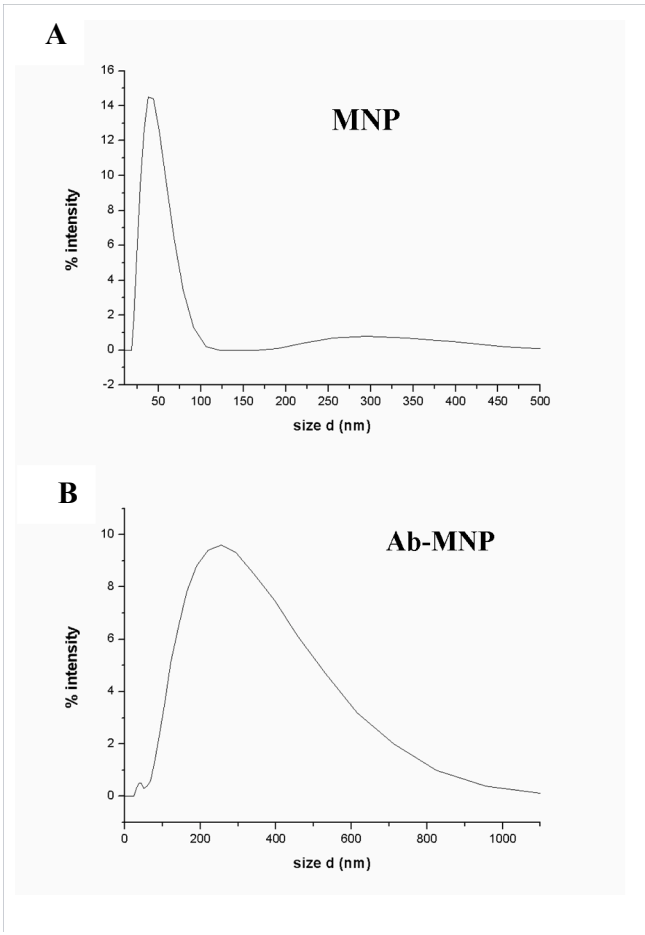

Fig. 3. Dynamic light scattering (DLS). A) DLS device shows the size distribution of nanoparticles unconjugated to antibodies and their size was estimated to be 44 nm which is consistent with the TEM. B) Shows the size distribution of nanoparticles conjugated to antibodies, which obtained their size 45–230 nm.

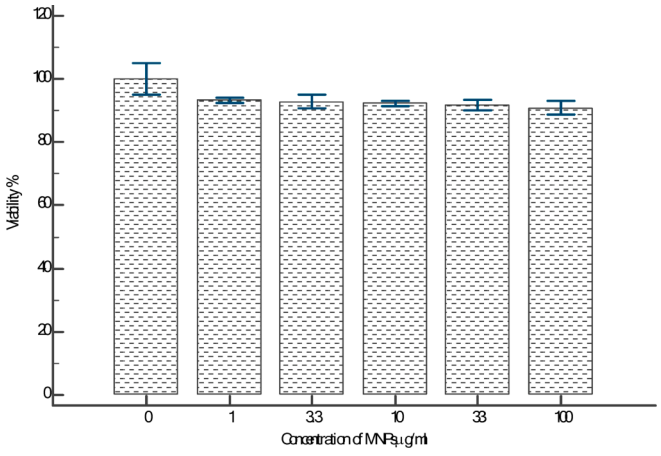

Fig. 4. Following the conjugating the anti-CD3 antibodies to MNPs, the MTS assay was employed to determine cytotoxicity MNP at 0, 1, 3.3, 10, 33 and 100 μg/mL concentrations.

2.3.1. Characterization

To determine its size and surface charge after coating the NPs, the sample was diluted with distilled water and a DLS, Zeta, and a TEM [42] of Technology was used to investigate the size of the nanoparticle core [43] as well as its shape and morphology. In addition, the MNP

Table 1
Assessment of the percentage of loaded antibodies on the surface of MNP.

Entry	MNP:A b	MNP (mg)	Antibody (μg)	CNBr (%)	EDC (%)
1	1:1	0.2	200	42	38
2	1:10	2	200	59	51
3	1:20	5	250	53	49

Table 2
The percentage of T CD3+ cells in bound fractions of CNBR and EDC method.

Entry	MNP: Ab	Antibody Concentration(μg/mL)	Mean number of bound cells whit CNBr	Mean number of bound cells whit EDC
1	1:1	4	302,000	**285,000**
		8	350,000	**320,000**
		12	405,000	**382,000**
2	10:1	4	420,000	**361,000**
		8	580,000	**430,000**
		12	420,000	**478,000**
3	20:1	4	287,000	**270,000**
		8	320,000	**290,000**
		12	362,000	**350,000**

crystalline structure was characterized through using X-ray diffraction (XRD) on a Holland Philips Xpert X-ray powder diffraction (XRD) diffractometer (CuK, radiation, $\lambda = 0.154056$ nm) at a scanning speed of 2°/min from 10 to 80° (2 θ). A powder-form sample was utilized in this regard. Further, vibrating-sample magnetometery (VSM) was exploited to determine the NPs' magnetic properties, prove their super-paramagnetism, and draw residual curve. The amount of the mass change caused by heating NPs, and more precisely that of the dextran coated with TGA was obtained [44-46]. Furthermore, the iron element concentration in the NPs was specified by using ICP-OE.

The MNPs were evaluated by using a KYKY EM-3200 TEM operated at a 26 kV accelerating voltage and fluorescence was measured by using an ELISA plate reader (Biotech, ELX 80.0, USA) and a fluorescent microscope (Nikon, Eclipse TE 2000-S, Japan) to assess the intensity of antibody.

2.3.2. Dynamic light scattering (DLS)

The hydrodynamic size, size distribution, and ζ-potential of prepared MNP were analyzed by applying DLS on a Zetasizer Nano ZS. Additionally, each diameter value was calculated by averaging the values related to three successive measurements. The higher and lower values demonstrate a very broad size distribution and more or less monodisperse particle size dispensation, respectively.

2.4. Assessing the bio-application of prepared MNPs

2.4.1. Isolation of viable peripheral blood mononuclear cells (PBMCs)

The blood sample was gently homogenized in heparin blood collection tube and diluted with PBS 1× (1:1). In addition, the volume of diluted cell suspension over was carefully layered and centrifuged at 400 *g* for 30 min at RT. Further, the supernatant leaving the mononuclear cell layer undisturbed at the interphase was aspirated. After transferring the mononuclear cell layer into a new tube, PBS1X (1:1 v/v) was added and centrifuged at 280 *g* for 8 min at RT. The supernatant was discarded and followed by resuspending the pellet in the favorable volume of flow cytometry buffer for surface and intracellular staining and counting the cells.

2.4.2. MTS assay

Briefly, 1×10^5 PBMC cells/well were cultured in DMEM-F12 does not contain phenols, treated by using the various concentrations of NP-conjugated antibodies (0, 1, 3.3, 10, 33, 100 μg/mL), and incubated for 24 h at 37 °C under 5% CO2 and 95% humidity. The PBMCs in Culture

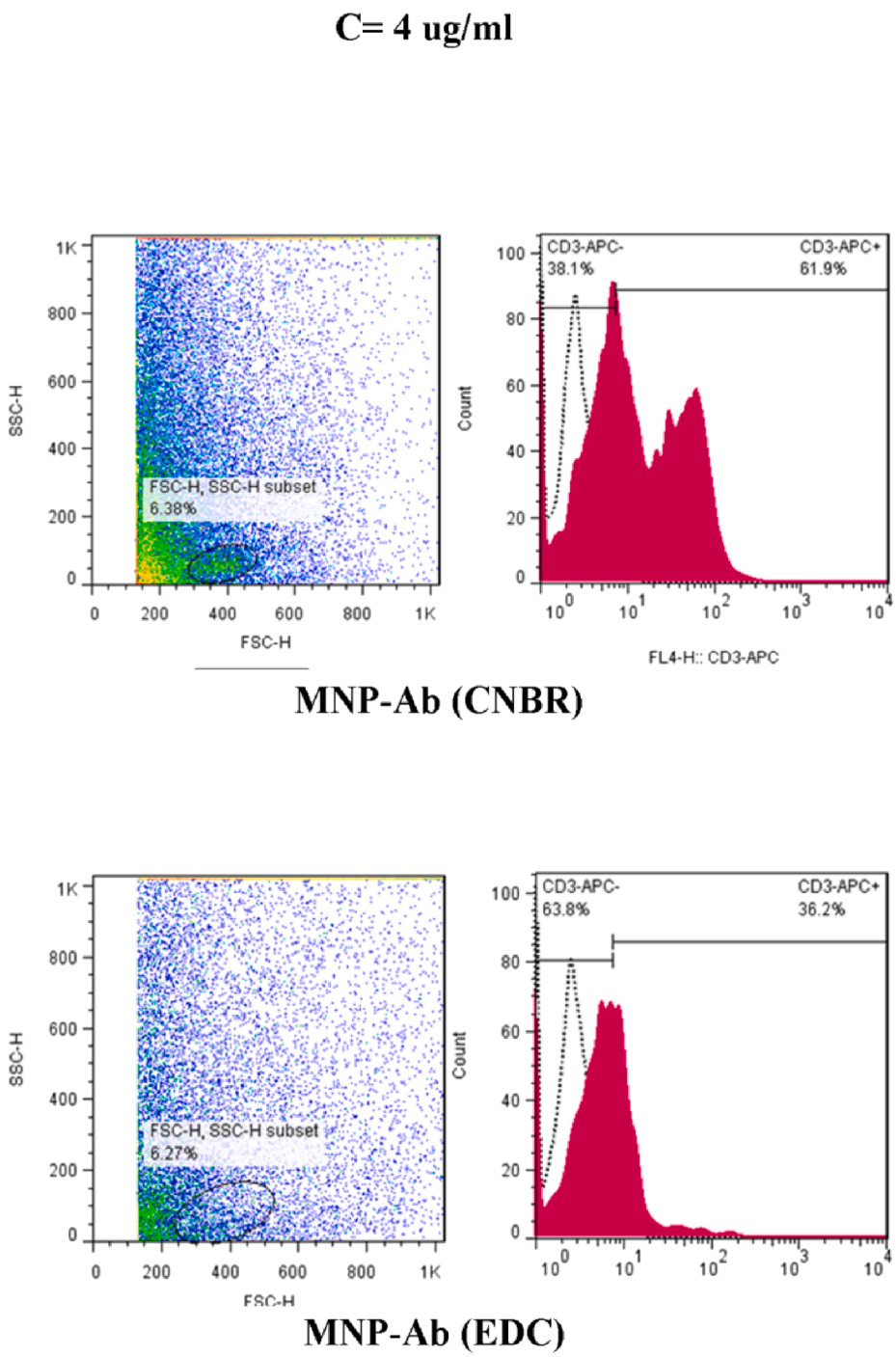

Fig. 5. Isolation of T CD3+ cells using anti-CD3-MNP conjugate. The histograms of flow cytometric analyses on the T CD3+ cells separated by MNP-Ab conjugates at various Ab concentrations in the conjugation ratio of 1:10 with MNP and Cell sorting of CD3+ T cells from PBMC by different Ab concentrations (4, 8, 12 μg/mL) of each anti-CD3-MNP conjugate. Displays the results of flow cytometry analysis on the T CD3 + cells labeled with MNP conjugated by CNBR compared to the EDC/NHS method. The results indicated that 80% of CD3+ T cells were respectively separated with MNP-CD3 by CNBR.

medium complete were thought out as the control. After incubation, MTS reagent (20 μg/mL) was added for 3 h. Then, they were examined by using a plate reader (Model ELx800, Bio-Tek Instruments, Winooki, USA) at 490 nm. The percentage of cell viability was calculated as follows.

$$\%\text{Viability} = (\text{mean OD test} - \text{mean OD MNP})/(\text{mean OD PBMCs} - \text{mean OD MNP}) \times 100$$

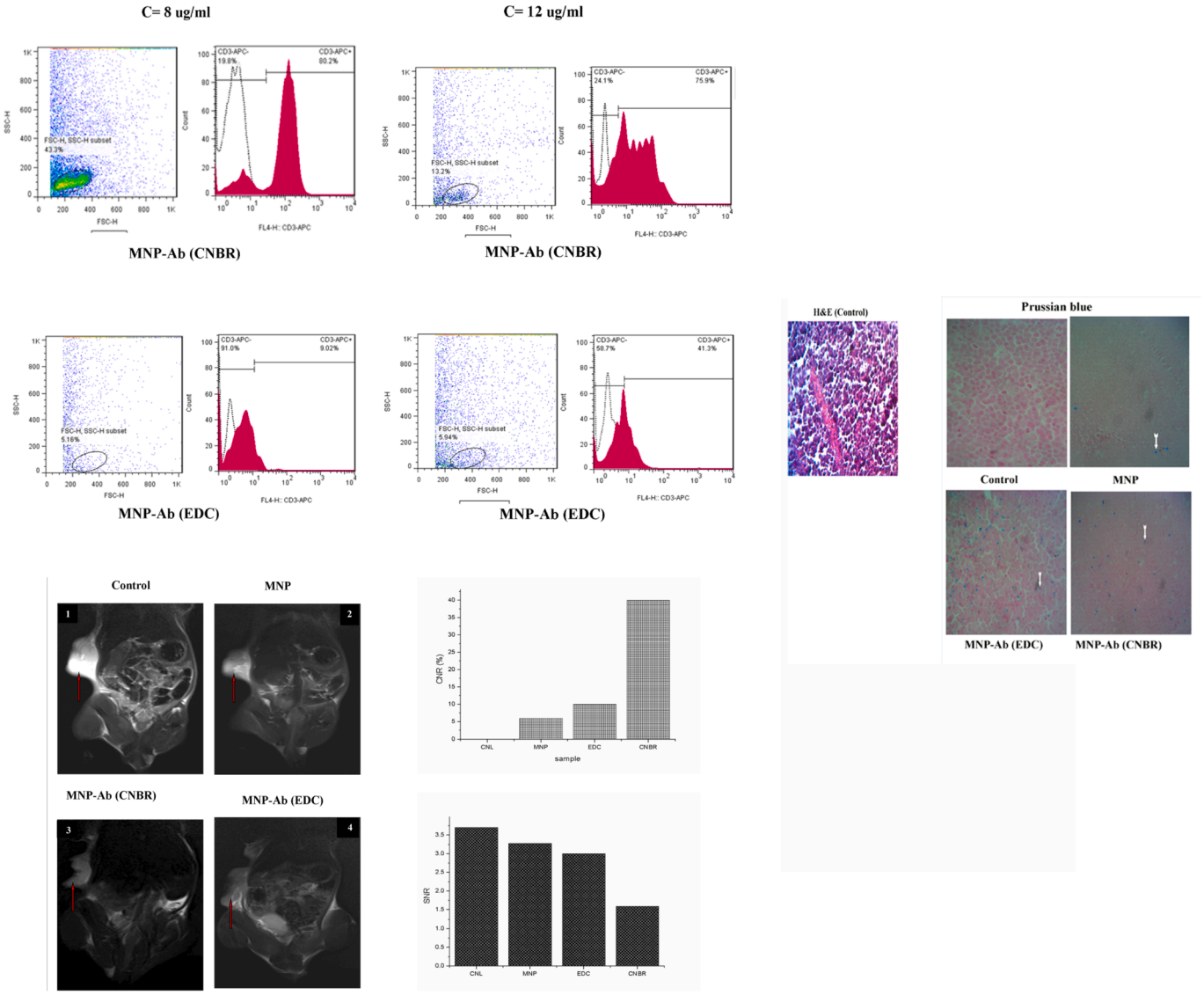

Fig. 6. Comparison of MRI images taken from NOG mice by different conjugation methods. 1) is a control group that has received a saline buffer and we do not see any signal in it. 2) Show that the unconjugated nanoparticles are received and we see a very weak signal. 3) Shows MRI result of antibody conjugated to iron oxide nanoparticles using cyanogen bromide method. Therefore, we see darker region than the control state in which no magnetic nanoparticle is injected (ie; white appearance). Here, it can be concluded that more intense dark contrast shows more uptake of the cyanogen bromide NP. 4) Antibody-conjugated nanoparticles received EDC/NHS method. In these images, the location of tumor is specified by arrows.

2.4.3. *Determination of the antibody amount conjugated with MNP-CD3*

The concentration of MNP-conjugated antibodies was measured by employing a BCA kit (Pierce ™ BCA protein assay kit, thermo science) at 572 nm based on the production instructions. Additionally, bovine serum albumin (BSA) was utilized as a standard protein to obtain a standard curve and total protein concentration in a sample was measured through using BCA assay. Furthermore, that of NP-conjugated antibody was obtained by considering a standard curve based on the BCA concentration. The same concentration of NPs was used as blanks.

The amount of conjugated antibody was calculated as follows.

$$\text{Percentage of conjugated antibody} = \text{antibody to MNPs/initial amount of Ab} \times 100$$

2.4.4. *Isolation of $CD3^+$ lymphocyte from PBMCs*

After purifying PBMCs, 1×10^6 cells were isolated and 60 μL of Fe_3O_4–CMD-conjugated antibodies was added at 4–12 μg/mL anti-CD3 Ab in pH = 7.2 and incubated for 20 min in the refrigerator. In addition, the cells were loaded into the MACS column and unlabeled cells were gathered. Further, the column was rinsed by adding 500 μL of PBS in three steps to minimize non-specific cell binding and remove excess

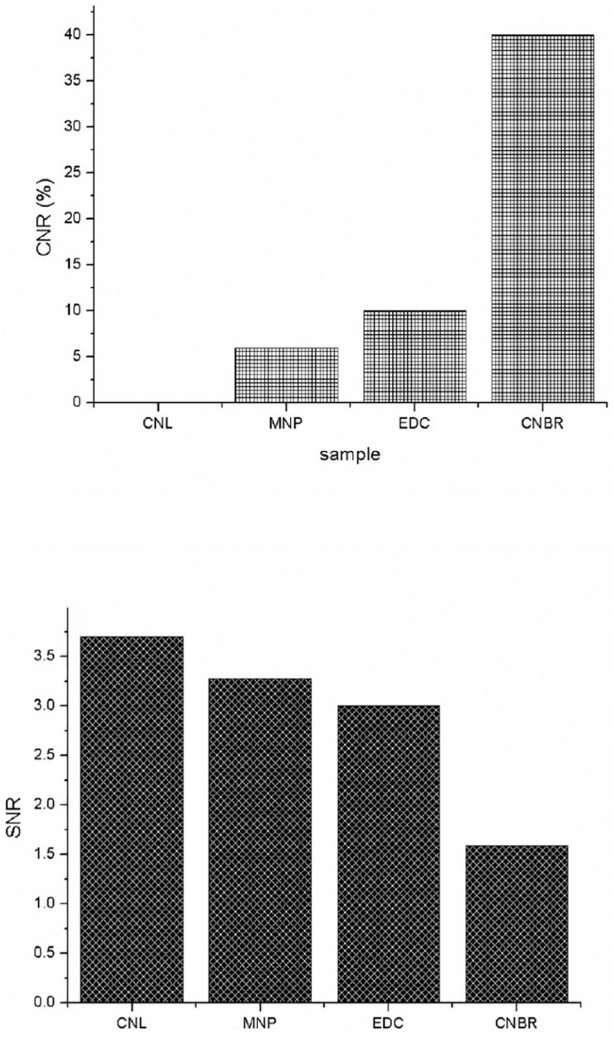

Fig. 7. Contrast to Noise Ratio (CNR) and Signal-to-Noise Ratio (SNR) analysis in the tumor of NOG mice.

NPs and antibodies. Furthermore, the contents of the column were emptied into a microtube through its detachment from the magnet by using a piston, and the cells were counted.

Following washing, the labeled cells were incubated in 90 μL of PBS −2% fetal bovine serum (FBS) staining buffer with 10 μL of APC, the cells were rinsed, re-suspended in 0.5 mL of PBS-FBS 2%, and analyzed. Finally, the frequency of TCD3 + cells was assessed by analyzing labeled cells.

2.5. Animal studies

The animal experimentation protocol in the current study was approved by the ethics committee of Tehran University of Medical Sciences. Male mice with 6–8 weeks NOD.Cg-Prkdcscid IL2rgtm1Sug (NOG) with the same body weight were obtained from the animal facilities of the Digestive Disease Research Institute of Tehran University of Medical Sciences. The mice were placed in a temperature control center for a 12-h period in a positive shelf of ambient temperature (23–21 °C) with separate ventilation. In the study, the relative humidity of 40–60% was, and sterile water and food were provided to the animals freely.

2.6. Tumor cell line preparation

For this purpose, Jurkat cell line was obtained from Pasteur Institute (Tehran, Iran) and cultured in RPMI-1640 medium with 10% FBS (Gibco, Fisher Scientific, Gothenburg, Sweden) (Bio-Idea, Tehran, Iran). Then, the cells were incubated at 37 °C under 5% CO2 and 95% humidity.

2.7. Inoculation

In this regard, 1×10^6 early passage Jurkat cells of tumor cell suspensions were subcutaneously injected into the right flank region of animals. One month later, the mice tumor tissues were harvested at the end of the MRI experiments for histological analysis. Then, the tumors were fixed in 10% buffered formalin and a part of the resected tumors was taken, stained with PB, and subjected to histological examination.

2.8. PB staining

PB staining was performed after sacrificing by barbiturate overdose. Following intravenous administration or direct inoculation, the tumors were fixed in paraformaldehyde and sections were embedded in paraffin for histochemical analyses. Additionally, iron was histologically detected through using PB and H & E staining method [47], and confirmed by a pathologist.

2.9. MRI imaging

MR imaging was performed for the mice that were fixed in a supine position by using a 3 T (Siemens, Prisma Germany) scanner with a high resolution standard transmit/receive 2 channel coils. Imaging parameters were TR = 4000 ms, TE = 85 ms, flip angel = 150°, FOV = 79 mm × 59 mm, slice thickness = 2 mm that was carry out in both coronal orientation using gradient echo T2.

2.10. Statistical analyses

SPSS16 software was utilized for analyses and the descriptive statistics for quantitative variables were expressed as mean ± SE. The normality of the data was determined through using Kolmogorov-Smirnov test and their mean was compared at different concentrations by using one-way ANOVA and bootstrap. Significance level was considered less than 0.05.

3. Results and discussion

The present study introduced a method to provide an optimal and cost-effective technique for the functionality of this bio-conjugate in two applications: The separation of $TCD3^+$ cells from PBMCs and ability of this conjugate to label lymphocytes. Further, EDC/NHS was used as a positive control and the performance of cyanogen bromide was compared. Based on the results, it generally was simple, rapid, and inexpensive method for cell fractionation, in which water is applied instead of organic solvents. Furthermore, a cheap linker was selected for conjugating NPs to antibodies, which was fast and available. The method utilizes the MNP beads attached to the specifically-targeted antibodies produced against cell surface antigens. In general, the coated MNP beads are stabilized well and considered as suitable for utilizing in the body, which can be appropriately digested or decomposed at a specific time and attached to the specifically-targeted antibodies produced against cell surface antigens. Thus, the use of a correct and optimal method for this connection can be beneficial and help to provide a suitable technique for separating the target cells from a set of heterogeneous ones. Fig. 1 represents the conjugation process of antibody to microbead, as well as their separation by using MACS. Finally, the fabricated MNP was characterized through using various techniques such as VSM, XRD, FT-IR, DLS, Zeta potential, and TEM.

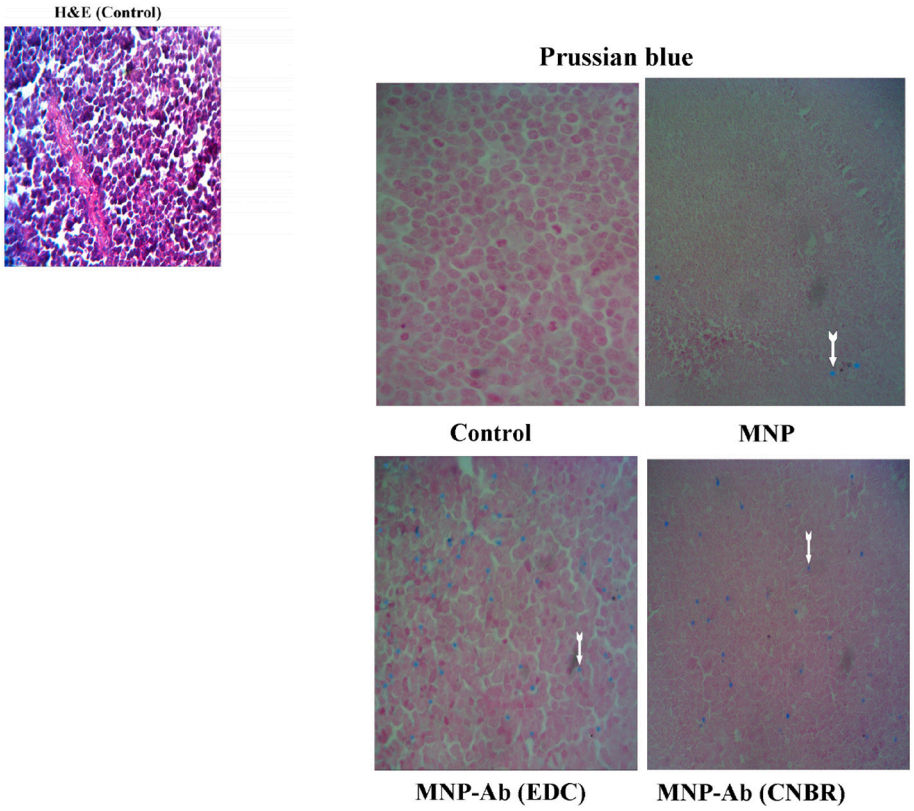

Fig. 8. Histopathological investigation of tumor in mice. a. the results of H & E staining demonstrated that the tumor mass of T cell was desired and the animal model was created correctly. b Based on the results, the CD3+ cells were co-localized with the PB-stained deposits in the joints of the mice infused with MNP-CD3, not MNP, which reflected the labeling specificity of MNP-CD3 in vivo (EDC/NHS as a positive control).

3.1. Characterization of the MNP3.1.1. XRD

The crystallinity and phase structure of the product were examined through using XRD pattern analysis. Based on the results in Fig. 2A, admissible matches were achieved for compounds, which indicate the presence of only one crystalline phase in the samples. In addition, the broaden peaks in XRD pattern suggested the small particle size of the product. All of the diffraction peaks for the synthesized CMD-coated Fe3O4 were very close to the values reported in the literature for JCPDS No. 001-7260. The mean crystallite diameter of the product was estimated by using Debeys-Scherrer equation as 13 nm which confirm TEM images.

3.1.1. FT-IR spectra

The attachment of CMD on Fe_3O_4 surface was established through FTIR spectroscopy. As shown in Fig. 2B, the peak at 3244 cm^{-1} corresponds to the O—H band of CMD and water. Additionally, the CH2 bond of CMD and carbonyl of asymmetric carboxyl group appear at 2923 and 1590 cm^{-1}, respectively. Bond was displaced due to the complexation of carbonyl group with the MNP surface (red shift). Further, the peaks at 1009 and 583 cm^{-1} are respectively related to the C—O band of CMD and Fe—O bond of MNPs.

3.1.2. Vibrating sample magnetometer (VSM)

The magnetic characteristic of MNPs was measured through using VSM. Fig. 2C displays the hysteresis loop of the NPs, which demonstrates that all of the MNPs are superparamagnetic at RT with no hysteresis. The size effect can be considered as a reason for reducing saturation. These NPs with their properties were critical in the biomedical field.

3.1.3. TEM &DLS

The morphological structure of the NPs was obtained by using a TEM (Fig. 2D). Based on the results, the mean core size of the NPs was determined 13 nm. The MNP size distribution was assessed before conjugating MNP to antibody and after using DLS device. As depicted in Fig. 3, the pre-conjugated MNP size is 18, which is in line with the images and size obtained from TEM. Additionally, the size of the MNPs conjugated to antibody was obtained 40–100 nm, which indicates an increase in MNP size after conjugation, and consequently the binding of antibody to MNPs.

Comparing the results of MNP surface charge before and after conjugation reflected an enhancement in the charge from −11 to −9 by adding antibodies to the surface of amino-MNPs, which is a proof of proper conjugation.

3.2. Assessment of the in vitro cytotoxicity of prepared MNPs

Following the conjugation of MNPs to the anti-CD3 antibody, MTS assay was employed to determine its cytotoxicity at 0, 1, 3.3, 10, 33, and 100 μg/mL concentrations. Based on the results in Fig. 4, no toxicity was observed up to 100 μg/mL concentration. After conjugating the antibody with MNPs, the concentration of the antibody conjugated to the CMD-coated Fe_3O_4 could be obtained through using a direct and undirected (Absorption reading at 280 nm) method (Table 1).

In the study, two variables were examined to obtain the optimal conditions for separating TCD3 + cells from the PBMCs generated by MNPs. In this regard, conjugation was performed in the different ratios of antibodies and NPs (1:1, 1:10, and 1:20). After specifying the most efficient ratio of MNPs to antibodies, the various concentrations of antibodies (4, 8, and 12 μg/mL) were tested. Based on the results, the more appropriate ratio for purity measurement was obtained 1:10 by determining the percentage of the antibody loaded on the MNP surface. Two factors of maximum yield (mean number of bound cells) and purity (percentage of TCD3 + cells in the bound fraction) were considered to

achieve the desired conditions for cell isolation. Thus, the ratio of 1:10 (MNP:Ab) with a concentration of 8 μg/mL was selected. Furthermore, all experiments were performed for EDC/NHS as a positive control. In addition, $CD3^+$ cells were separated by using the prepared MNP-Ab conjugate. Further, the number of cells was counted inbound fractions by using a neobar lam and flow cytometry analysis was performed by APC-conjugated anti-CD3 antibody (Biolegend, USA). The number of $TCD3^+$ cells in the bound (positive selection) fractions was determined through using both EDC/NHS and cyanogen bromide methods at all conjugation ratios (Table 2). Fig. 5 demonstrates the histograms of flow cytometric analyses on the T CD3+ cells separated by MNP-Ab conjugates at various Ab concentrations in the conjugation ratio of 1:10.

3.3. Labeling efficacy

Fig. 5 displays the results of flow cytometry analysis on the T CD3 + cells labeled with MNP conjugated by CNBR compared to the EDC/NHS method. The results indicated that 80% of CD3+ T cells were respectively labeled with MNP-CD3.

4. In vivo MRI and prussian blue (Pb)

The sections of tumor were stained to discover if the migrated (to the peripheral part of tumors) iron-positive cells were true of human origin, leading to low signal intensity on MRI. Additionally, the mice were sacrificed for histological examinations at the end of the MRI experiments in order to allow the correlation with the imaging results. Further, MRI imaging was performed among four groups including one receiving the conjugated antibodies conjugated by using cyanogen bromide and EDC/NHS which infused with MNPs, and the control which was not inoculated than after 30 min (Fig. 6). Signal-to-Noise Ratio (SNR) and Contrast to Noise Ratio (CNR) analysis in the tumor of NOG mice noticeably decreased and increased, respectively, and in comparison with control mice that did not receive bioconjugation, showing that the CD3+ cells were co-localized with the PB-stained deposits in the joints of the mice infused with MNP-CD3, not MNP, which reflects the labeling specificity of MNP-CD3 in-vivo (EDC/NHS as a positive control) (Fig. 7).

The MR images exhibited areas in the tumor with low signal intensities compared to the control group, which were the active site of iron positive CD3 migration. Furthermore, the results of H & E staining demonstrated that the tumor mass of T cell ALL was desired and the animal model was created correctly (Fig. 8). However, those of PB staining represented that multiple iron-positive cells were present in the tumors of the mice injected with labeled CD3 cells (CNBr and EDC/NHS) although the spot number in the cyanogen bromide method was more than that in EDC/NHS one. Despite the lack of investigation about the changes of the tumors' signal intensity with labeled and unlabeled cells, according a general agreement, all of the tumors with administered labeled CD3 cells exhibit low signal intensity areas along the periphery of the tumors corresponding to PB-positive cells.

5. Limitation of the study

The limitations of the study include lacking to compare CNBr method with the different conjugation techniques, requiring further research regarding the accuracy of this method, needing to examine more mice in different groups, and developing the method only in the form of exploration. Therefore, the study should be complemented by characterizing number xenograft models.

6. Conclusion

Today, various methods can be applied for conjugating antibodies to MNPs although a need for cost-effective and simpler conjugation techniques is felt. Cyanogen bromide conjugation is considered as one of the methods, on which no comprehensive and good study has been conducted so far. In this study, MNPs were conjugated to anti-CD3 antibodies by using cyanogen bromide, followed by characterizing the method. Based on the results, conjugation was successful. In addition, bio-conjugate was biologically evaluated, and its functionality, as well as the toxicity of bio-conjugation was respectively assessed. The produced bio-conjugates can have two applications in the medical field, including cell sorting, as one of the most important usages in adoptive cell therapy such as CAR-T cell therapy, as well as developing targeted contrast agents for MRI imaging. The present study examined the functionality of the bio-conjugate in the above-mentioned applications. In fact, it assessed cell sorting by isolating lymphocytes from blood cells in vitro, as well as the ability of this conjugate to label lymphocytes in vivo through MRI and PB staining.

CRediT authorship contribution statement

N. Moradi, S. Mohamadnejad, H, Ghafouri: Conceptualization, Methodology, Writing- Original draft preparation. H. Ghafouri, A. Oghabian: Supervision. H. Delavari, H.Ghafouri S. Mohamadnejad, A. Oghabian: Reviewing and Editing. Negin Pournouri: MRI data analysis.

Acknowledgements

Thankfully acknowledge for the cooperation of Tehran University of Medical Sciences for supporting this project numbered 97-01-30-38105, the Department of Cellular and Molecular Imaging Research Center (RCSTIM), and National Brain Mapping Lab for their cooperation whit this research, as well as Professor Ali Mostafaie from the Medical Biomedical Research Center (MBRC) in Kermanshah for his contribution to my education. Also, the authors thank the Research Council of University of Guilan for the financial support to this study.

References

[1] X. Lin, A.O. Beringhs, X. Lu, Applications of nanoparticle-antibody conjugates in immunoassays and tumor imaging, AAPS J. 23 (2) (2021) 1–16, https://doi.org/10.1208/s12248-021-00561-5.
[2] M.M. Cardoso, I.N. Peca, A.C.A. Roque, Antibody-conjugated nanoparticles for therapeutic applications, Curr. Med. Chem. 19 (19) (2012) 3103–3127.
[3] P. Dennler, E. Fischer, R. Schibli, Antibody conjugates: from heterogeneous populations to defined reagents, Antibodies 4 (3) (2015) 197–224.
[4] P.M.S.D. Cal, G.J.L. Bernardes, P.M.P. Gois, Cysteine-selectivereactions for antibodyconjugation, Angew. Chem. Int. Ed. 53 (40) (2014) 10585–10587.
[5] H.J. Kim, et al., Therapeutic application of drug-conjugated HER2 oligobody (HER2-DOligobody), Int. J. Mol. Sci. 21 (9) (2020) 3286.
[6] I.H. El-Sayed, X. Huang, M.A. El-Sayed, Surface plasmon resonance scattering and absorption of anti-EGFR antibody conjugated gold nanoparticles in cancer diagnostics: applications in oral cancer, Nano Lett. 5 (5) (2005) 829–834.
[7] A. Juan, F.J. Cimas, I. Bravo, A. Pandiella, A. Ocaña, C. Alonso-Moreno, An overview of antibodyconjugatedpolymericnanoparticles for breastcancertherapy, Pharmaceutics 12 (9) (2020) 802.
[8] K. Mu, et al, Monoclonal antibody–conjugated superparamagnetic iron oxide nanoparticles for imaging of epidermal growth factor receptor–targeted cells and gliomas, Mol. Imaging 14 (5) (2015) 2015–7290.
[9] M.H. Jazayeri, H. Amani, A.A. Pourfatollah, H. Pazoki-Toroudi, B. Sedighimoghaddam, Various methods of gold nanoparticles (GNPs) conjugation to antibodies, Sens. Bio-sens. Res. 9 (2016) 17–22.
[10] H. Yao, F. Jiang, A. Lu, G. Zhang, Methods to design and synthesize antibody-drug conjugates (ADCs), Int. J. Mol. Sci. 17 (2) (2016) 194.
[11] K. Tripathi, J.D. Driskell, Quantifying bound and active antibodies conjugated to gold nanoparticles: a comprehensive and robust approach to evaluate immobilization chemistry, ACS Omega 3 (7) (2018) 8253–8259.
[12] R.A. Sperling, W.J. Parak, Surface modification, functionalization and bioconjugation of colloidal inorganic nanoparticles, Philos. Trans. R. Soc. A Math. Phys. Eng. Sci. 368 (1915) (2010) 1333–1383.
[13] A. Kumar, S. Mao, N. Dimasi, C. Gao, Design and validation of linkers for site-specificpreparation of antibody-drugconjugatescarryingmultipledrugcopiespercysteineconjugationsite, Int. J. Mol. Sci. 21 (18) (2020) 6882.
[14] Z. Rashid, F. Shokri, A. Abbasi, M. Khoobi, A.-H. Zarnani, Surface modification and bioconjugation of anti-CD4 monoclonal antibody to magnetic nanoparticles as a highly efficient affinity adsorbent for positive selection of peripheral blood T CD4+ lymphocytes, Int. J. Biol. Macromol. 161 (2020) 729–737.
[15] S.B. Merriam, Qualitative Research and Case Study Applications in Education. Revised and Expanded From"Case Study Research in Education", ERIC, 1998.

[16] C. Kim, J.F. Galloway, K.H. Lee, P.C. Searson, Universal antibody conjugation to nanoparticles using the Fcγ receptor I (FcγRI): quantitative profiling of membrane biomarkers, Bioconjug. Chem. 25 (10) (2014) 1893–1901.
[17] D.A. Goodwin, C.F. Meares, M. Osen, Biological properties of biotin-chelate conjugates for pretargeted diagnosis and therapy with the avidin/biotin system, J. Nucl. Med. 39 (10) (1998) 1813.
[18] R.P. Haugland, W.W. You, Coupling of antibodies with biotin, in: Avidin-Biotin Interactions, Springer, 2008, pp. 13–23.
[19] Pournoori Negin, Tehran University of Medical Sience, 2018.
[20] J.M. Kavran, D.J. Leahy, Coupling antibody to cyanogen bromide-activated sepharose, Methods Enzymol. 541 (2014) 27.
[21] L. Jin, et al., CD70, a novel target of CAR T-cell therapy for gliomas, Neuro-Oncology 20 (1) (2018) 55–65.
[22] M. Pillai, M.M. Davies, F.C. Thistlethwaite, Delivery of adoptive cell therapy in the context of the health-care system in the UK: challenges for clinical sites, Ther. Adv. Vaccines Immunother. 8 (2020), 2515135520944355.
[23] Y.-P. Jiang, et al., CLT030, a leukemic stem cell–targeting CLL1 antibody-drug conjugate for treatment of acute myeloid leukemia, Blood Adv. 2 (14) (2018) 1738–1749.
[24] M.J. Frank, A. Huang, S.-W. Tang, R.S. Negrin, S. Hsiao, E.H. Meyer, A novelantibody-cellconjugationmethod to enhancecellulartherapies for the treatment of hematologicalmalignancies, Blood 130 (Supplement 1) (2017) 1532.
[25] Z. Wang, Z. Wu, Y. Liu, W. Han, New development in CAR-T cell therapy, J. Hematol. Oncol. 10 (1) (2017) 1–11.
[26] B.M. Davies, et al., Quantitative assessment of barriers to the clinical development and adoption of cellular therapies: a pilot study, J. Tissue Eng. 5 (2014), 2041731414551764.
[27] B.H. Villas, Flow cytometry: an overview, Cell Vis. J. Anal. Morphol. 5 (1) (1998) 56–61.
[28] M.K. Brakke, Density gradient centrifugation: a new separation technique1, J. Am. Chem. Soc. 73 (4) (1951) 1847–1848.
[29] Y. Zhu, et al., Proteome profiling of 1 to 5 spiked circulating tumor cells isolated from whole blood using immunodensity enrichment, laser capture microdissection, nanodroplet sample processing, and ultrasensitive nanoLC–MS, Anal. Chem. 90 (20) (2018) 11756–11759.
[30] J. Bauer, Advances in cell separation: recent developments in counterflow centrifugal elutriation and continuous flow cell separation, J. Chromatogr. B Biomed. Sci. Appl. 722 (1–2) (1999) 55–69, https://doi.org/10.1016/S0378-4347(98)00308-9.
[31] M.V. Golovanov, CRC Press, Boca Raton, FL, 1994.
[32] H. Wen, et al., Enhancement of membrane stability on magnetic responsive hydrogel microcapsules for potential on-demand cell separation, Carbohydr. Polym. 157 (2017) 1451–1460.
[33] I. Antal, et al., D, l-lysine functionalized Fe3O4 nanoparticles for detection of cancer cells, Colloids Surf. B Biointerfaces 163 (2018) 236–245.
[34] A.K. Gupta, M. Gupta, Synthesis and surface engineering of iron oxide nanoparticles for biomedical applications, Biomaterials 26 (18) (2005) 3995–4021.
[35] S.G. Grancharov, et al., Bio-functionalization of monodisperse magnetic nanoparticles and their use as biomolecular labels in a magnetic tunnel junction based sensor, J. Phys. Chem. B 109 (26) (2005) 13030–13035.
[36] B. Yoo, M.D. Pagel, An overview of responsive MRI contrast agents for molecular imaging, Front. Biosci. 13 (3) (2008) 1733–1752.
[37] J.-H. Lee, et al., Artificially engineered magnetic nanoparticles for ultra-sensitive molecular imaging, Nat. Med. 13 (1) (2007) 95–99.
[38] S.-W. Chou, Y.-H. Shau, P.-C. Wu, Y.-S. Yang, D.-B. Shieh, C.-C. Chen, In vitro and in vivo studies of FePt nanoparticles for dual modal CT/MRI molecular imaging, J. Am. Chem. Soc. 132 (38) (2010) 13270–13278.
[39] G. Chen, et al., miR-146a inhibits cell growth, cell migration and induces apoptosis in non-small cell lung cancer cells, PLoS One 8 (3) (2013), e60317.
[40] W. Zeng, X. Wang, P. Xu, G. Liu, H.S. Eden, X. Chen, Molecular imaging of apoptosis: from micro to macro, Theranostics 5 (6) (2015) 559.
[41] C. Decaestecker, O. Debeir, P. Van Ham, R. Kiss, Can anti-migratory drugs be screened in vitro? A review of 2D and 3D assays for the quantitative analysis of cell migration, Med. Res. Rev. 27 (2) (2007) 149–176.
[42] X. Chen B. Zheng H. Liu, "Optical and digital microscopic imaging techniques and applications in pathology", Anal. Cell. Pathol., 34, no. 1, 2, pp. 5–18, 2011.
[43] W. Brown, J. Zhao, Adsorption of sodium dodecyl sulfate on polystyrene latex particles using dynamic light scattering and zeta potential measurements, Macromolecules 26 (11) (1993) 2711–2715.
[44] M. Khalkhali, K. Rostamizadeh, S. Sadighian, F. Khoeini, M. Naghibi, M. Hamidi, The impact of polymer coatings on magnetite nanoparticles performance as MRI contrast agents: a comparative study, DARU J. Pharm. Sci. 23 (1) (2015) 45.
[45] J. Kang, G. Yeom, H. Jang, J. Oh, C.-J. Park, M.-G. Kim, Development of replication protein A-conjugated gold nanoparticles for highly sensitive detection of disease biomarkers, Anal. Chem. 91 (15) (2019) 10001–10007.
[46] H. Jahangirian, K. Kalantari, Z. Izadiyan, R. Rafiee-Moghaddam, K. Shameli, T. J. Webster, A review of small molecules and drug delivery applications using gold and iron nanoparticles, Int. J. Nanomedicine 14 (2019) 1633.
[47] K. Rowatt, R.E. Burns, S. Frasca Jr., D.M. Long, A combination Prussian blue–hematoxylin and eosin staining technique for identification of iron and other histological features, J. Histotechnol. 41 (1) (2018) 29–34.